



AFRL-AFOSR-VA-TR-2023-0229

Increasing Pulse Length and Repetition Rate of Relativistic Magnetrons and MILO

**Schamiloglu, EdI
UNIVERSITY OF NEW MEXICO
1700 LOMAS BLVD NE
ALBUQUERQUE, NM,
US**

**12/15/2022
Final Technical Report**

DISTRIBUTION A: Distribution approved for public release.

Air Force Research Laboratory
Air Force Office of Scientific Research
Arlington, Virginia 22203
Air Force Materiel Command

REPORT DOCUMENTATION PAGE

PLEASE DO NOT RETURN YOUR FORM TO THE ABOVE ORGANIZATION.

1. REPORT DATE 20221215	2. REPORT TYPE Final	3. DATES COVERED	
		START DATE 20190915	END DATE 20220914
4. TITLE AND SUBTITLE Increasing Pulse Length and Repetition Rate of Relativistic Magnetrons and MILO			
5a. CONTRACT NUMBER	5b. GRANT NUMBER FA9550-19-1-0225	5c. PROGRAM ELEMENT NUMBER 61102F	
5d. PROJECT NUMBER	5e. TASK NUMBER	5f. WORK UNIT NUMBER	
6. AUTHOR(S) Edl Schamiloglu			
7. PERFORMING ORGANIZATION NAME(S) AND ADDRESS(ES) UNIVERSITY OF NEW MEXICO 1700 LOMAS BLVD NE ALBUQUERQUE, NM US			8. PERFORMING ORGANIZATION REPORT NUMBER
9. SPONSORING/MONITORING AGENCY NAME(S) AND ADDRESS(ES) Air Force Office of Scientific Research 875 N. Randolph St. Room 3112 Arlington, VA 22203		10. SPONSOR/MONITOR'S ACRONYM(S) AFRL/AFOSR RTB1	11. SPONSOR/MONITOR'S REPORT NUMBER(S) AFRL-AFOSR-VA-TR-2023-0229
12. DISTRIBUTION/AVAILABILITY STATEMENT A Distribution Unlimited: PB Public Release			
13. SUPPLEMENTARY NOTES			
14. ABSTRACT The relativistic magnetron is the most compact and efficient high power microwave (HPM) source. The MILO (Magnetically Insulated Line Oscillator) is an HPM source that is more efficient from a systems standpoint – it does not require an external magnetic field. Two main ideas are being pursued in computation and experiments: 1) A relativistic magnetron with diffraction output (MDO) powered by a split cathode (we moved away from using a magnetic mirror to the split cathode as it offers tremendous advantages and is simpler). 2) The use of carbon nanotube cathode woven carpets in relativistic magnetrons and the MILO. This topic is an on-going collaboration with Dr. Steven Fairchild (AFRL/RX) who spent time at UNM for this collaboration and Drexel University and a spin-off company Dexmat. This final report presents the results of theory, particle-in-cell simulations, experiments, and plasma diagnostics that advanced our understanding of the MDO and MILO. It also summarizes our interactions with other performers, provides a management summary, and lists the journal articles resulting from the research.			
15. SUBJECT TERMS			
16. SECURITY CLASSIFICATION OF:		17. LIMITATION OF ABSTRACT	18. NUMBER OF PAGES
a. REPORT U	b. ABSTRACT U	c. THIS PAGE U	UU 21
19a. NAME OF RESPONSIBLE PERSON JOHN LUGINSLAND			19b. PHONE NUMBER (Include area code) 000-0000

REPORT DOCUMENTATION PAGE

PLEASE DO NOT RETURN YOUR FORM TO THE ABOVE ORGANIZATION.

1. REPORT DATE	2. REPORT TYPE	3. DATES COVERED	
November 17, 2022	Final Technical Report	START DATE	END DATE
		September 15, 2019	September 14, 2022

4. TITLE AND SUBTITLE
Increasing Pulse Length and Repetition Rate of Relativistic Magnetrons and MILOs

5a. CONTRACT NUMBER	5b. GRANT NUMBER	5c. PROGRAM ELEMENT NUMBER
	FA9550-19-1-0225	
5d. PROJECT NUMBER	5e. TASK NUMBER	5f. WORK UNIT NUMBER

6. AUTHOR(S)
Schamiloglu, Edl and Portillo, Salvador

7. PERFORMING ORGANIZATION NAME(S) AND ADDRESS(ES)	8. PERFORMING ORGANIZATION REPORT NUMBER
University of New Mexico Department of Electrical and Computer Engineering: Pulsed Power, Beams, and Microwaves Laboratory MSC01 1100 211 Terrace St. NE Albuquerque, NM 87131-0001	ES-AFOSR-FR-02022-11

9. SPONSORING/MONITORING AGENCY NAME(S) AND ADDRESS(ES)	10. SPONSOR/MONITOR'S ACRONYM(S)	11. SPONSOR/MONITOR'S REPORT NUMBER(S)
Air Force Office of Scientific Research 875 North Randolph Street, Suite 325 Arlington, VA 22203	AFOSR	

12. DISTRIBUTION/AVAILABILITY STATEMENT
Approved For Public Release; Distribution Unlimited

13. SUPPLEMENTARY NOTES

14. ABSTRACT
The relativistic magnetron is the most compact and efficient high power microwave (HPM) source. The MILO (Magnetically Insulated Line Oscillator) is an HPM source that is more efficient from a systems standpoint – it does not require an external magnetic field. Two main ideas are being pursued in computation and experiments and are summarized in this Final Report:

- 1) A relativistic magnetron with diffraction output (MDO) powered by a split cathode with electrons in a squeezed state;
- 2) The use of carbon nanotube cathode woven carpets in relativistic magnetrons and the MILO, and the further advancement of the MILO through particle-in-cell simulations.

15. SUBJECT TERMS
High power microwaves, HPM, high power RF, HPRF, relativistic magnetron, relativistic magnetron with diffraction output, MDO, magnetically insulated line oscillator, MILO, cathodes, split cathode, squeezed state

16. SECURITY CLASSIFICATION OF:			17. LIMITATION OF ABSTRACT	18. NUMBER OF PAGES
a. REPORT	b. ABSTRACT	c. THIS PAGE		
U	UU	UU	None	21

19a. NAME OF RESPONSIBLE PERSON	19b. PHONE NUMBER (Include area code)
Edl Schamiloglu	505-277-6095



**AFOSR Final Technical Report
Grant FA9550-19-1-0225
September 15, 2019 – September 14, 2022**

Lead Organization: The Regents of the University of New Mexico

Technical Point of Contact: Edl Schamiloglu, Distinguished Professor, edls@unm.edu

Administrative Point of Contact: Timothy Wester

Contract & Grant Administrator, Tel. (505) 277-1264, twester@unm.edu

Grant Title: Increasing Pulse Length and Repetition Rate of Relativistic Magnetrons and MILO

Technical Area: Plasma and Electro-Energetic Physics

AFOSR PO: John Luginsland

TABLE OF CONTENTS

TABLE OF CONTENTS	3
ABSTRACT	4
I. DETAILED RESEARCH SUMMARY	5
Task 1 – Ultra-High-Efficiency Relativistic Magnetron with Diffraction Output (MDO)	5
Background	5
Split Cathode	5
Pulsed Power Modification and Simulations	7
Experimental Results – UNM	9
Experimental Results – Technion	11
Diocotron Instability	13
Task 2 – The Magnetically Insulated Line Oscillator (MILO)	14
Introduction	14
Experimental MILO Research at UNM	15
Computational Research	18
Supplemental Task – SOARD-Funded Collaboration with Dr. Rossi, INPE, Brazil	19
Conclusions	20
II. MANAGEMENT SUMMARY	20
III. JOURNAL PUBLICATIONS	20
IV. PATENT APPLICATIONS	21

ABSTRACT

The relativistic magnetron is the most compact and efficient high power microwave (HPM) source. The MILO (Magnetically Insulated Line Oscillator) is an HPM source that is more efficient from a systems standpoint – it does not require an external magnetic field. Two main ideas are being pursued in computation and experiments:

1) A relativistic magnetron with diffraction output (MDO) powered by a split cathode (we moved away from using a magnetic mirror to the split cathode as it offers tremendous advantages and is simpler).

2) The use of carbon nanotube cathode woven carpets in relativistic magnetrons and the MILO. This topic is an on-going collaboration with Dr. Steven Fairchild (AFRL/RX) who spent time at UNM for this collaboration and Drexel University and a spin-off company Dexmat.

This final report presents the results of theory, particle-in-cell simulations, experiments, and plasma diagnostics that advanced our understanding of the MDO and MILO. It also summarizes our interactions with other performers, provides a management summary, and lists the journal articles resulting from the research.

I. DETAILED RESEARCH SUMMARY

This project at the University of New Mexico (UNM) has two primary tasks: 1) development of an ultra-high-efficiency relativistic magnetron with diffraction output (MDO), and 2) development of new cathodes for use on a MILO. This report describes technical achievements on these two tasks through the end of the grant period. These two primary tasks have subtasks as indicated below:

1. Ultra-High-Efficiency Relativistic Magnetron with Diffraction Output (MDO)
 - Collaboration with The Technion
2. The Magnetically Insulated Line Oscillator (MILO)
 - Cathode development
 - Spectroscopic studies

Task 1 – Ultra-High-Efficiency Relativistic Magnetron with Diffraction Output (MDO)

Background

In our original proposal we were planning on studying the MDO with virtual cathode (VC) and the MDO with magnetic mirror. However, in FY20, Q3 we decided to abandon this approach for the following reasons:

1. Experiments at UNM with the MDO and VC resulted in some RF generation, but mostly dead shorts and a considerable amount of concomitant bremsstrahlung radiation generation. Particle-in-cell (PIC) simulations had indicated that this approach was promising. However, in experiments, the electric field stress in the radial A-K gap far exceeded the threshold for breakdown so this approach was not viable and was abandoned.
2. Implementing a magnetic mirror as proposed would require i) additional magnetic field-producing coils, ii) an additional power supply, and would result in a heavier, less efficient system, making it less attractive for future mobile platforms.

At about the same time, we initiated a collaboration with Yakov Krasik and John Leopold at The Technion in Haifa, Israel (Technion is funded by ONR Global). This collaboration led to an extremely fruitful direction, resulting in the development and implementation of what we call the **split cathode**.¹ The split cathode is an elegant, lightweight, passive (no power needed) solution to completely suppress axial leakage current from the MDO.

Split Cathode

Figure 1 presents an idealized simulation of how the split cathode works (without being in the MDO's interaction regime for simplification). The split cathode consists of a series of annular cathode emitters made out of carbon nanotubes embedded in epoxy located external to the MDO

¹J.G. Leopold, M.S. Tov, S. Pavlov, V. Goloborodko, Ya.E. Krasik, A. Kuskov, D. Andreev, and E. Schamiloglu, "Experimental and Numerical Study of a Split Cathode Fed Relativistic Magnetron," J. Appl. Phys., vol. 130, 034501-1-7 (2021).

interaction region. A small diameter central rod connects the emitters to the downstream reflector. An electron beam is injected into the interaction region and, instead of forming a VC (as we had proposed earlier – here we do not form a VC), the electrons flow downstream, are reflected from the reflector and flow upstream, are reflected from the cathode and flow downstream, and so on. (Not requiring a VC enables us to significantly increase the radial A-K gap, resulting in much lower electric field stress on the anode and avoiding electrical breakdown.) Over several transit times, the electrons gradually lose energy, forming a “squeezed state,” as originally described by Ignatov and Tarakanov.² Figure 2 presents MAGIC PIC simulations that show the evolution of the squeezed state for the geometry in Fig. 1.

Figure 3 presents a photograph of the final machined, anodized split cathode at UNM. An identical set was produced and shipped to NSWC DD. Figure 4 presents a photograph of the split cathode assembly installed on the MDO at UNM.

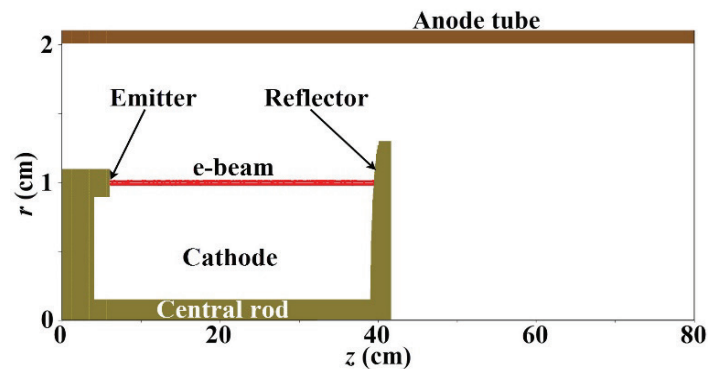


Figure 1. A cross section of an axially symmetric arrangement of a split cathode made up from an emitter, a reflector, and a central rod placed coaxially inside an anode tube. The beam snapshot is at 6 ns.

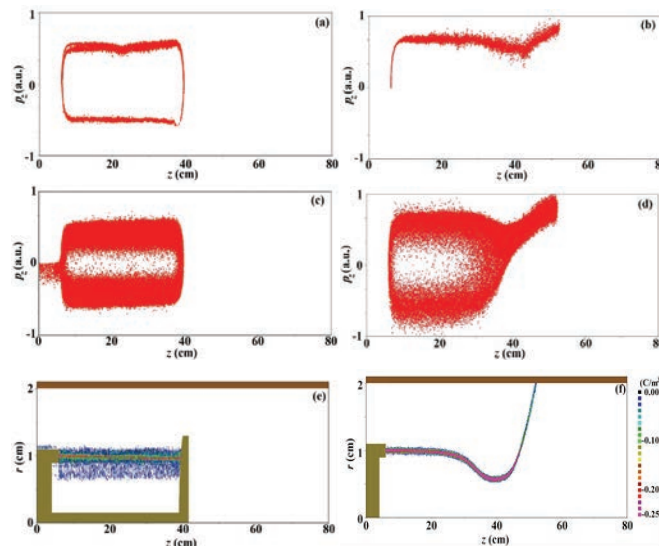


Figure 2. $[z, p_z]$ phase space for the reflector [(a) at 6 ns and (c) at 45 ns] and for the magnetic mirror [(b) at 6 ns and (d) at 45 ns] cases. Electron charge density distribution at 45 ns for the reflector (e) and the magnetic mirror (f) cases. The color bar is the same for (e) and (f).

²A.M. Ignatov and V.P. Tarakanov, “Squeezed State of High-Current Electron Beam,” *Phys. Plasmas* 1, 741 (1994).



Figure 3. Photograph of the machined, anodized split cathode assembly (left) at UNM. Photograph showing the carbon nanotube emitters (right).

Pulsed Power Modification and Simulations

Before we proceeded with experiments at UNM, the modified PI-110A accelerator was upgraded. The liquid resistors were replaced with solid state resistors, as shown in Fig. 5. This led to more consistent performance on a shot-to-shot basis. In addition, comprehensive end-to-end PIC simulations were performed using ICEPIC that included the pulsed power section. Figure 6 shows a comparison of a SolidWorks drawing of the MDO with the end-to-end ICEPIC model of it. Figure 7 presents a Spice model of the MDO's pulsed power network.

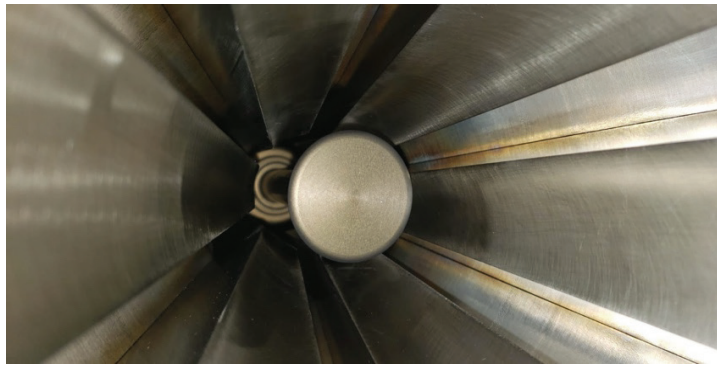
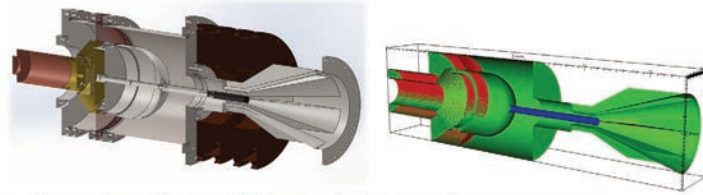


Figure 4. Photograph of the split cathode assembly installed on the MDO at UNM.



Figure 5. Photograph of the PI-110A accelerator used for MDO experiments showing solid state resistors in place.

ICEPIC Model Mimics Experimental Setup



- Proper boundary conditions at the input and output ports
- Careful consideration of emission parameters and surfaces
- Mesh size for correct solution and adequate simulation time

Figure 6. SolidWorks drawing of the MDO (left) compared to its end-to-end ICEPIC model (right).

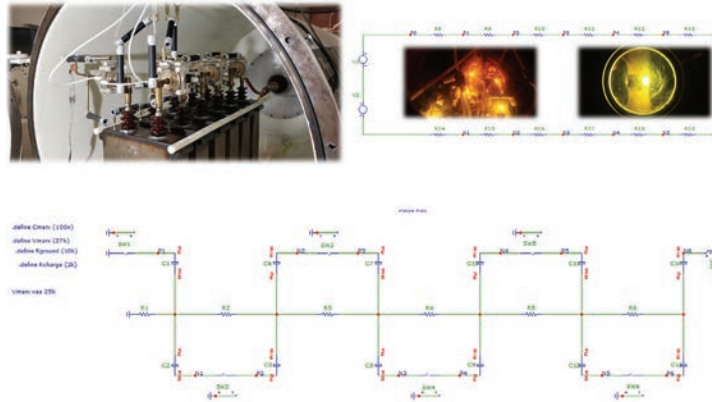


Figure 7. Spice model of the MDO's pulsed power network.

Figure 8 presents a comparison of experimental waveforms with the ICEPIC and Spice models for the MDO on the PI-110A.

Modeling is an iterative process of comparing experimental and simulation results and improving model

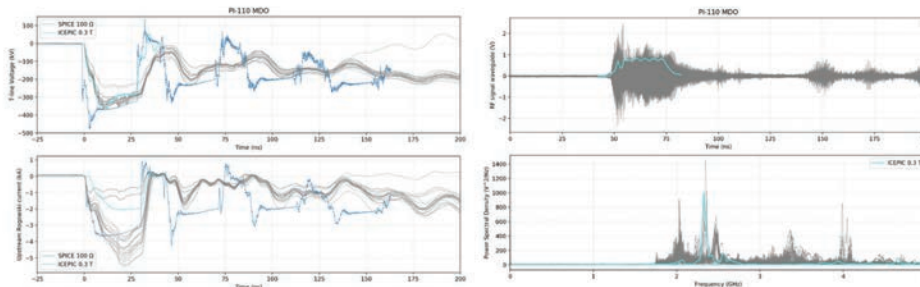


Figure 8. Comparison of the experimental waveforms (gray) with ICEPIC (light blue) and Spice simulations (dark blue) (courtesy Dmitrii Andreev, Ph.D. Dissertation).

Experimental Results – UNM

Experiments were performed at UNM on the PI-110A accelerator. Figure 9 presents a photograph of the accelerator ready for experiments with the MDO and split cathode. Figure 11 presents a summary of the first type of shots. The axial magnetic field was set at 0.29 T, and the accelerator was charged to achieve an output of 250 kV. Figure 10(a) shows the time vs. amplitude plots of current (green), voltage (red), and the RF field (blue) detected by a free space D-dot sensor. The peak voltage of the main pulse shows about 250 kV and the current has an initial spike where electrons are emitted and then reflected. Later, when electron charge accumulates in the interaction space, the mode forms and RF is generated. After about 150 ns, the main pulse drops, yet the current keeps increasing, meaning the electrons are shorting to the anode. Meanwhile, the load voltage drops because of this short. Figure 10(c) shows a time-frequency plot for this shot, which confirms the idea that no meaningful frequency is produced from the reflected signal. Figure 10(b) shows the FFT of the signal, which indicates some mode competition in the main pulse. The RF has two main frequencies at 2.53 GHz and 2.61 GHz, which correlate with the π mode according to simulations from Section 3.5.3.



Figure 9. Photograph of the PI-110A as it is set-up for MDO experiments with a split cathode.

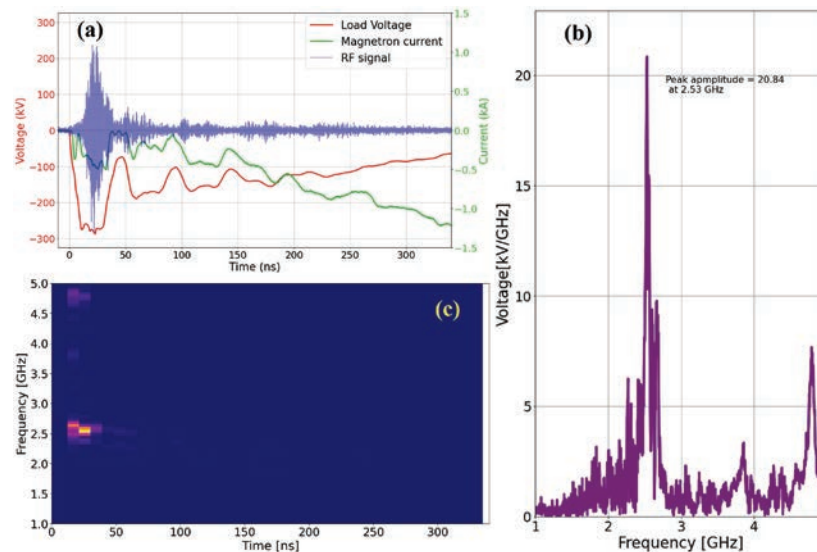


Figure 10. MDO with split cathode result case 1. (a) Voltage (red), current (green), and RF (blue) signals as a function of time. (b) FFT of the RF signal. (c) Time-frequency plot of the RF signal.

The second case is shown in Figure 11, where the RF pulse is produced during the reflection of the voltage pulse. Similar to the first case, the primary pulse only lasts about 30 ns at 200 kV, but the RF is produced much later when the reflected voltage reaches 150 kV. In this case the RF signal exists for 150 ns, which is much longer than the main pulse. The frequency content, as shown in Figure 11 (b), shows less mode competition and one major frequency at 2.2 GHz. It is suspected that this frequency corresponds to the $2\pi/3$ mode of the MDO.

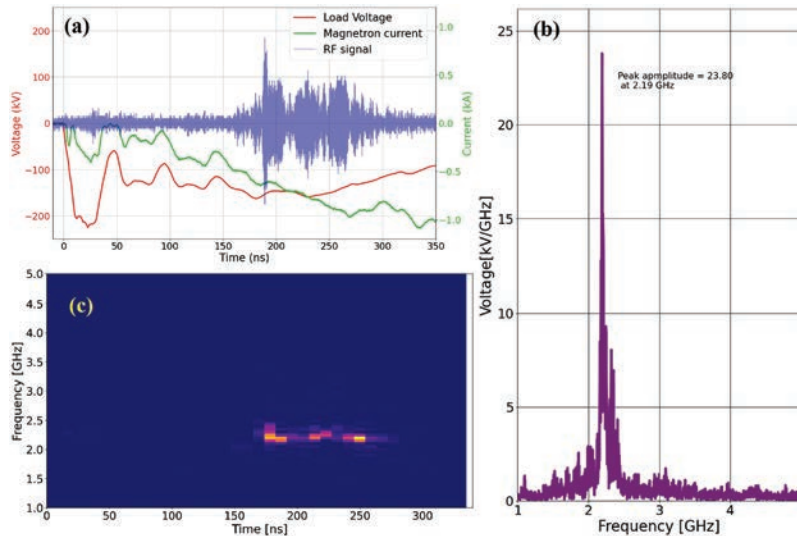


Figure 11. MDO with split cathode result case 2. (a) Voltage (red), current (green), and RF (blue) signals as a function of time. (b) FFT of the RF signal. (c) Time-frequency plot of the RF signal.

Finally, Figure 12 demonstrates the third case where the RF signal is present for over 200 ns. Similar to the previous case, electrons do not start the mode at high voltages and the modulation starts when the reflected voltage drops to about 150 kV. The frequency content suggests some mode competition, but the majority of the signal is generated at 2.2 GHz.

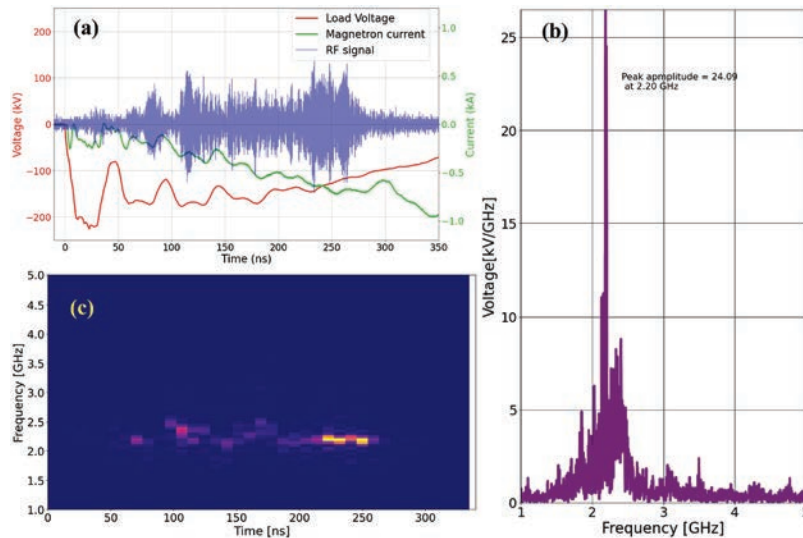


Figure 12. MDO with split cathode result case 3. (a) Voltage (red), current (green), and RF (blue) signals as a function of time. (b) FFT of the RF signal. (c) Time-frequency plot of the RF signal.

UNM experiments showed some interesting results. The input voltage of the major signal was too high in some cases to start the mode, but the frequency content of the mode was much better on average. In most cases, the reflected voltage signal was acting as the voltage source and produced much longer RF pulses, but at the cost of mode competition.

Experimental Results – Technion

Researchers at The Technion also performed several experiments with the split cathode that was jointly designed with UNM. The geometry of their magnetron differed from the UNM A6 MDO, but the working principle remains the same.^{3,4} The first experiments were performed on a magnetron structure without an output cavity. Figure 13 shows a comparison of different cathodes in the magnetron: solid cathode, solid cathode with reflector, and finally the split cathode. With the solid cathode without the reflector, the electric field has low amplitude and is generated during the interval 25-150 ns, while the input signal is over 300 ns long. This behavior is a sign of high leakage current in the system. The second case partially resolves this behavior and the amplitude of the RF is much higher; however, the pulselength of the electric field is similar to the first case. Figure 16(d) shows the input current in the system increasing while the RF signal decays. This behavior is explained by A-K gap closure.

When the physical cathode is removed from the interaction region, as is the case for the split cathode, the RF signal exists for the entire duration of the voltage pulse. The mode looks to be consistent, yet slightly shifting frequencies as time progresses, as shown in Figure 13(i). Figure 14 shows the estimated average microwave power. The results clearly exemplify the advantage of the split cathode when compared to the solid cathode for long input pulse operation.

The experiment described above was performed on a magnetron structure with no output cavity. The electric field was measured inside of one of the cavities using a B-dot. The next experiment was performed on a magnetron with separated anode segments and a split cathode.⁶ The segmented anode segments facilitated rapid penetration of a fast magnetic field.

Figure 15 shows the electric field that was measured at the magnetron output and also displays the correlation between microwave generation and the anode current in the system. As shown before, the split cathode-driven magnetron demonstrates some frequency shift as the voltage pulses progresses, and this behavior still needs to be investigated.

In summary, the split cathode completely eliminates axial leakage current and facilitates long pulse magnetron operation.

³J. Leopold, M.S. Tov, S. Pavlov, V. Goloborodko, Y.E. Krasik, A. Kuskov, D. Andreev, and E. Schamiloglu, “Experimental and Numerical Study of a Split Cathode Fed Relativistic Magnetron,” *J. Appl. Phys.*, vol. 130, 034501 (2021).

⁴Y.E. Krasik, J. Leopold, Y. Hadas, Y. Cao, S. Gleizer, E. Flyat, Y. Bliokh, D. Andreev, A. Kuskov, and E. Schamiloglu, “An Advanced Relativistic Magnetron Operating with a Split Cathode and Separated Anode Segments.” *J. Appl. Phys.*, vol. 131, 023301 (2022).

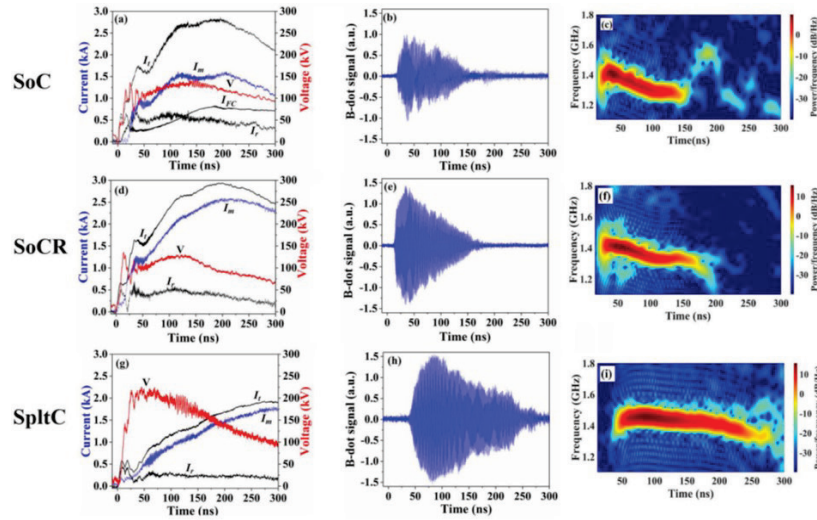


Figure 13. Summary of results from The Technion comparing cathodes: solid cathode (top), solid cathode with a reflector (middle), and the split cathode (bottom).⁵

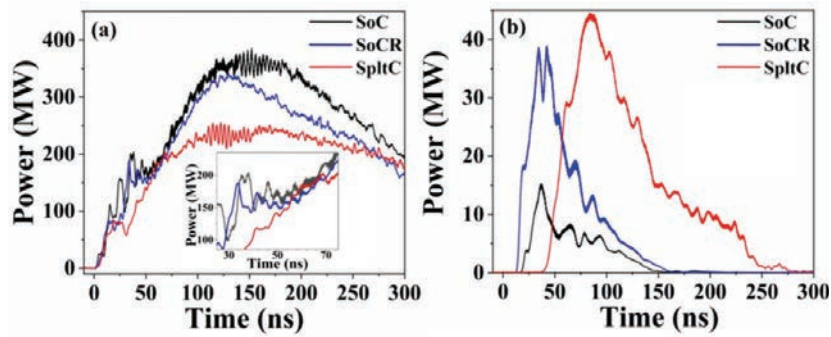


Figure 14. (a) The experimental input power (the insert in (a) is an enlarged view of the time interval 25-75 ns); (b) the average output power for the three cathode configurations tested.⁵

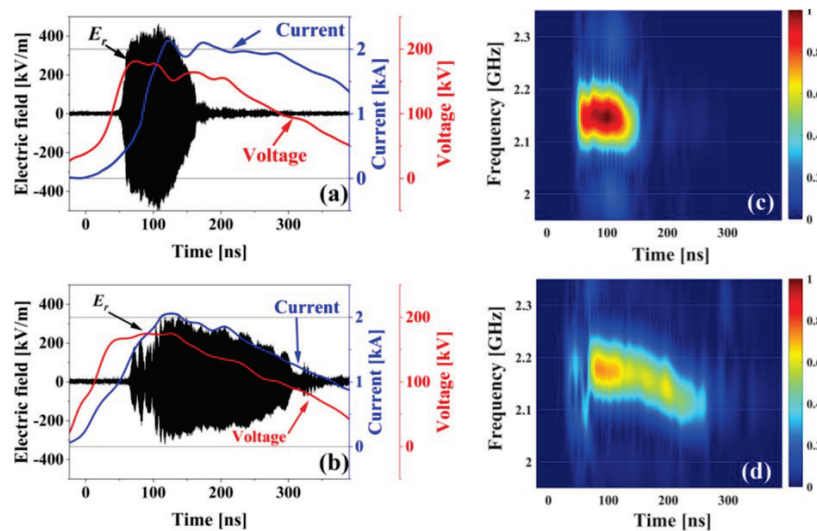


Figure 15. Typical waveforms of the voltage and current for magnetron with separate anode sections for (a) a solid cathode, (b) split cathode, and the time-frequency plots for the electric field signals in (a) and (b), respectively.⁶

Diocotron Instability

In this section we present the results of experiments and theoretical modeling which confirm the presence of periodic diocotron bunching of an electron cloud present in the potential well in a split cathode coaxial diode. This bunching can affect the mode which develops in the corresponding magnetron. We believe it can also be exploited to decrease the time for start-of-oscillations in relativistic magnetrons.

Experiments were carried out using the same experimental setup at The Technion described previously and with specific details shown in Figure 16.

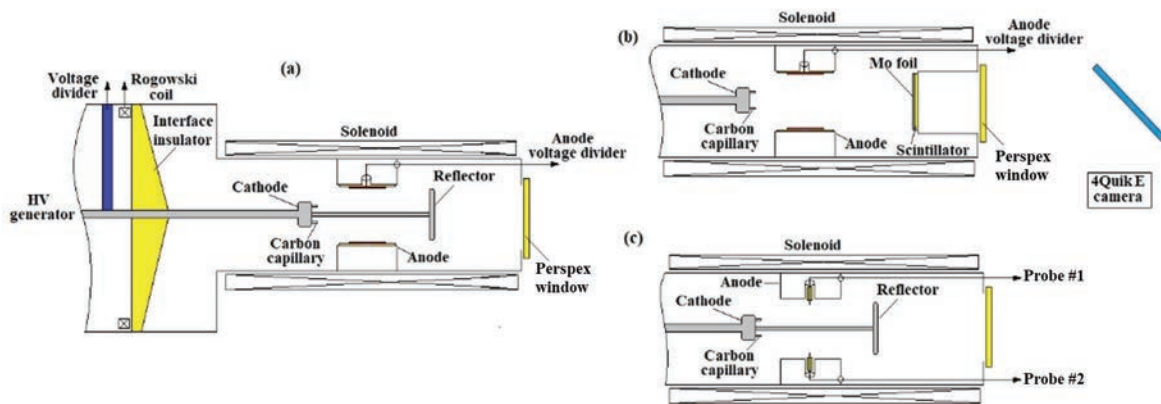


Figure 16. The experimental setup for (a) a wire grid reflector, (b) to record the beam in the absence of the reflector and rod and (c) with the probes #1 and #2.

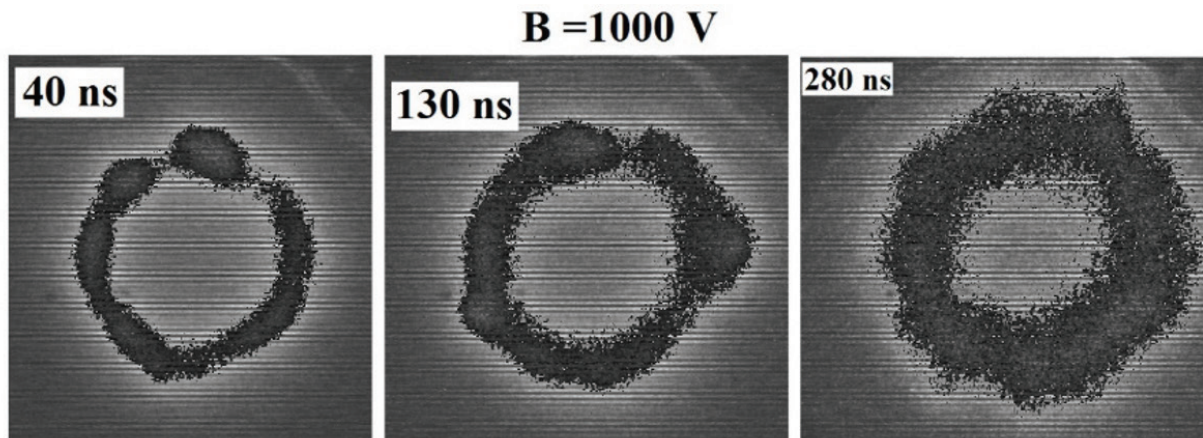


Figure 17. Framing images of luminescence appearing on a plastic scintillator due to the interaction of the electron beam with a 127- μm -thick Ta foil placed in front of the scintillator. The frame duration is 1.2 ns with a magnetic field 8 kG.

The existence of the diocotron instability in a split cathode geometry is confirmed by high frequency oscillations observed on the probe signals shown, for example, in Figure 18 together with the voltage and current waveforms. Experiments with probes #1 and #2 were carried out in

three configurations: (a) the split cathode; (b) no reflector and rod; and (c) no reflector but rod present. In all these cases, high frequency oscillations were observed in the probe signals.

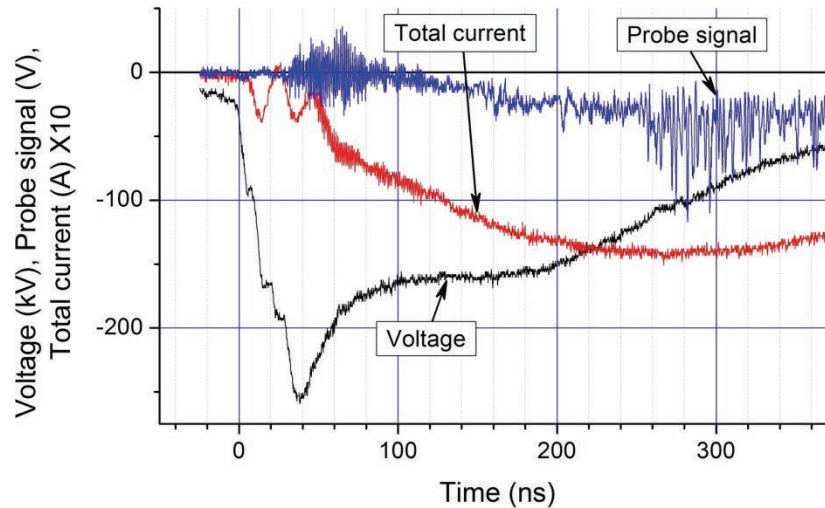


Figure 18. The probe signal, voltage, and current waveforms for the split cathode configuration, magnetic field 8 kG.

The theoretical model and data analyses have been submitted for publication to *Phys. Plasmas* and has just been accepted.

The experiments presented in this section with a split cathode in a magnetron-like geometry show the appearance of high frequency oscillations of the azimuthally rotating electron charge cloud. Wavelet analyses of these fast oscillations show that there is a correlation between these fast oscillating signals. A theoretical model of a squeezed electron state is considered and the results of this model agree with the experimentally obtained rotation frequency and its temporal behavior indicating the existence of a periodic diocotron instability. We believe that this instability can lead to faster turn on of the MDO. We anticipate further investigations of this instability as part of an overall effort investigating sources for higher frequency generation. Our preliminary findings have been submitted for publication⁵ and was just accepted.

Task 2 – The Magnetically Insulated Line Oscillator (MILO)

Introduction

Our principal goal during this sponsored research was to develop a deeper understanding of the problems faced by gigawatt class HPM, more specifically those that affect the MILO. If one could think of the optimum HPM crossed field source a couple of things would immediately come to mind. First, the need to make a source capable of high energy delivery, one that can deliver high peak power but do so for long pulse periods. Second this ideal source would be capable of generating energy at different frequencies on command – different narrowband as well as broadband spectra – with a goal to couple as much energy as possible onto the target being interdicted – it would find the best coupling path to the electronic target. Fairly straightforward, long pulses with as much energy as possible at the right frequency spectrum to maximize effects on target.

⁵Y.P. Bliokh, Ya.E. Krasik, J.G. Leopold, and E. Schamiloglu, “Observation of the Diocotron Instability in a Diode with a Split Cathode,” submitted to *Phys. Plasmas* (2022).

Digging down a bit though quickly leads us to a myriad of problems leading to the inability to achieve these goals. The dreaded gap closure or radiation collapse due to neutral desorption and resultant ionization of these neutrals that in turn neutralizes the incoming electron beam and thus stops the radiation production. These neutrals come from the electrodes, cathode and anode structures. And thus, our focus was a multipronged experimental and computational approach to understand the physics of cathode plasmas and ultimately mitigate these. We had an idea on the frequency tunability or adjustability that we felt would bypass all the work being done on MILOs utilizing two different regions with different cavity sizes by Chinese and Indian researchers. Our approach to this was completely computational. Our idea to alter the discrete LCR values of the MILO called for the use of computational techniques as we could not possibly build multiple versions of a MILO.

This portion of the final report then details these efforts, one I believe to be quite successful, and the other a work in progress. We did submit three patent applications, established strong collaborations, and laid the groundwork for additional development – the physics of neutral desorption and the ultimate effect on incident beam is nontrivial but we made some headway on this.

Experimental MILO Research at UNM

Often touted as a benefit, and it really is a benefit, is the high current of a MILO that leads to magnetic insulation to obviate the need for an external magnetic field. This means very large currents on the order of 20-30 kA for a 1 GHz device. The faster this current is developed, the better it is as otherwise the electron beam prior to magnetic insulation is hitting the anode at multiple locations, heating it and thereby releasing neutrals which in turn are ionized and radiation collapse occurs. If we are to have a long pulse HPM MILO we need cathodes capable of low outgassing, free of high Z molecules which can lead to highly ionized states in the AK gap and that turn on very fast. In order to measure these quantities UNM developed, as part of this grant, the capability to spatially and temporally measure the ionization in the AK gap, not just type but density and direction. But first what cathode to use? This fortuitously led to a deep collaboration with Dr. Steve Fairchild of AFRL/RX WPAFB in Ohio. Dr. Fairchild has been developing these wet spun weaved cathodes in collaboration with UK universities as well as with various small business here in the U.S.. He provided various cathode geometries for us to work with as we worked with them to understand how these emitters turned on, how long they lasted and yes how many neutrals these emitted. This partnership led to additional collaboration with Dexmat, a small concern out of Houston specializing in carbon nanotube (CNT) manufacturing and with the functional fabric department at Drexel University specializing in woven techniques for these CNT loops. UNM provided the pulsed power and the atomic physics expertise. We utilized our Lobo Linear Transformer Driver (LTD) cavity, originally meant for radiographic physics at the Nevada test site and now a near perfect driver for low impedance loads.

Our work supported by this grant then focused on measuring plasmas at various points in the AK gap by taking spectrographic snapshots of these. This grant allowed us to develop this spectrographic capability based on a coherent fiber array comprised of 15 fibers coupled to an advanced 500 mm spectrometer and an intensified CCD.

Figure 19 shows the geometry of our experimental apparatus and an image of the LOBO LTD firing these loads. The LOBO LTD is capable of delivering energy for approximately 300-400 ns with a sub-100 ns risetime. This makes it a nearly perfect surrogate for an HPM device that allows us to characterize these novel cathodes in the 100's ns timescale. Critical to our work was the development of a spatially resolved spectroscopic system. The LOBO LTD generates copious amounts of unintended electromagnetic energy and thus we cannot put our diagnostics adjacent to the accelerator. Under the auspices of this grant we developed a fiber array resistant to damage from UV light. This coherent fiber array is approximately 20 meters long and delivers the spatially resolved spectra to a spectrometer inside a faraday cage. The particulars of this spectrometry system are detailed in Figure 20.

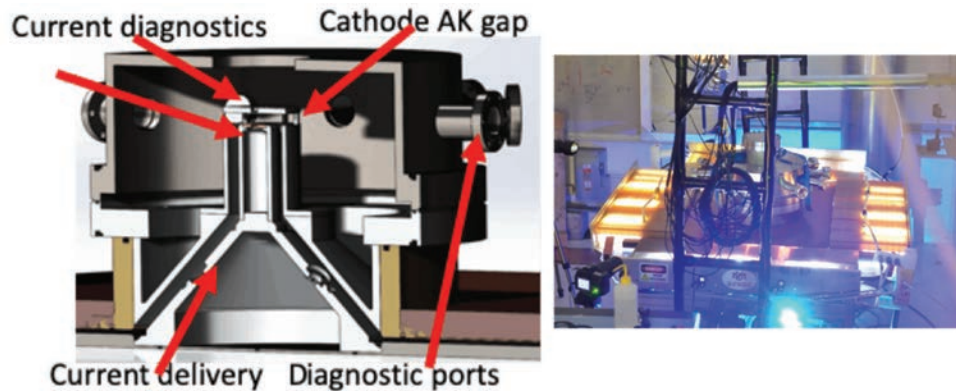


Figure 19. Left: Cutaway drawing of UNM's experimental chamber, showing multiple diagnostic viewports; Right: Photograph of the LOBO LTD firing and delivering energy into the load.

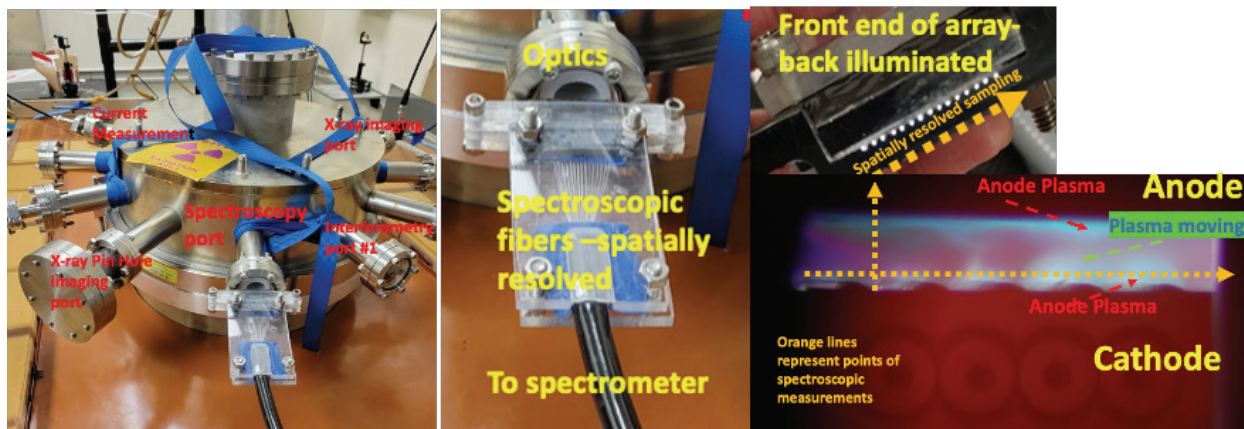


Figure 20. UNM experimental layout for measuring cathode plasmas. The left hand image shows the diagnostic ports, labels show the specific diagnostic. Center image shows our bespoke VIS coherent fiber array. Visible in the image are the imaging optics used to bring light to the individual fibers. The top right image shows the spatially resolved fibers as they are back illuminated, and the bottom image shows how these fibers are used to measure spatially resolved plasmas.

Figure 21 shows a large area configuration of the experimental apparatus. Figure 22 is a composite image of various cathode material and geometries fired during the period of performance of this grant. The last image of Figure 22 shows a time resolved evolution of a cathode turning on. Figure 23 shows a series of spectra taken from one of the cathodes clearly showing ionized hydrocarbons.

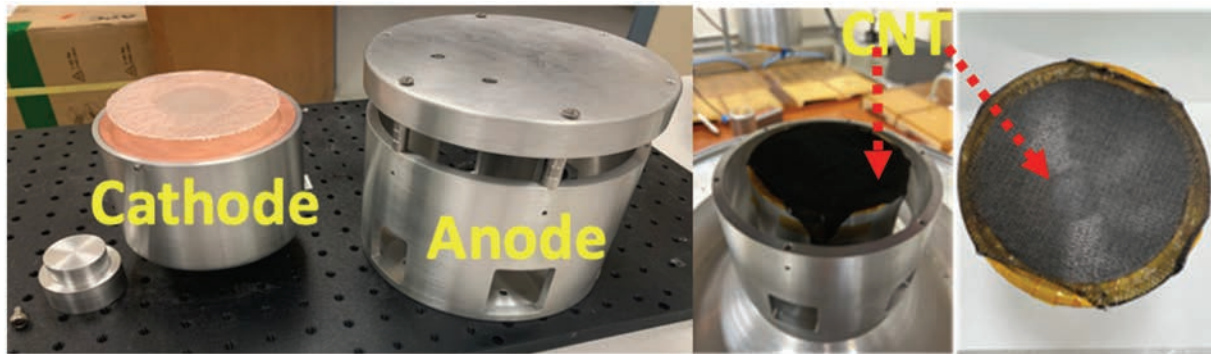


Figure 21. Typical hardware and assembly of a CNT cathode fired on the LOBO LTD. The left image shows the cathode holder next to the anode assembly. The latter can hold various anode materials although it was not possible to carry out the latter experiments with materials other than Al. The two far right images show the CNT cathode in place.

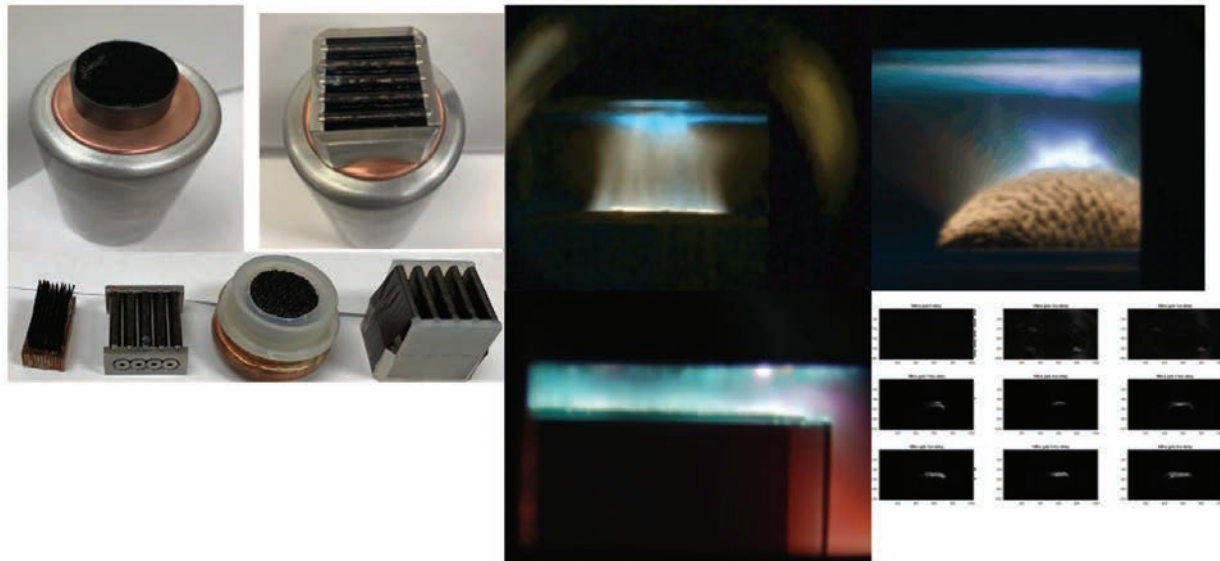


Figure 22. A photographic composite of various cathodes fired during this period of performance. The right had images show different cathode geometries taken by an open shutter camera. The pretty blue light corresponds to hydrocarbons borne both in the anode as well as in the cathode regions. The last set of images is a time resolved series showing cathode turn to full emission. Shown here only for emphasis as it is critical that the temporal evolution of the plasmas also be captured. At the time the image was taken the camera was quantum limited and, hence, the poor contrast.

The takeaway from these experiments is that we are finally measuring the neutral desorption, albeit only from cathodes and we are able to do so spatially resolved across the AK gap. We calculate densities via Stark Broadening to be on the order of $2.5 \times 10^{14}/\text{cm}^3$. On the material performance front, we found that the cathodes did indeed readily turn on and that we could build these to a somewhat large size of 10 cm diameter. Additional work by Drexel promises even larger cathodes. Although the material turns on readily and provides high current densities, we found that

outgassing or neutral desorption was a critical issue that needs to be address. Dr. Fairchild and our group are in discussions on how to mitigate this.

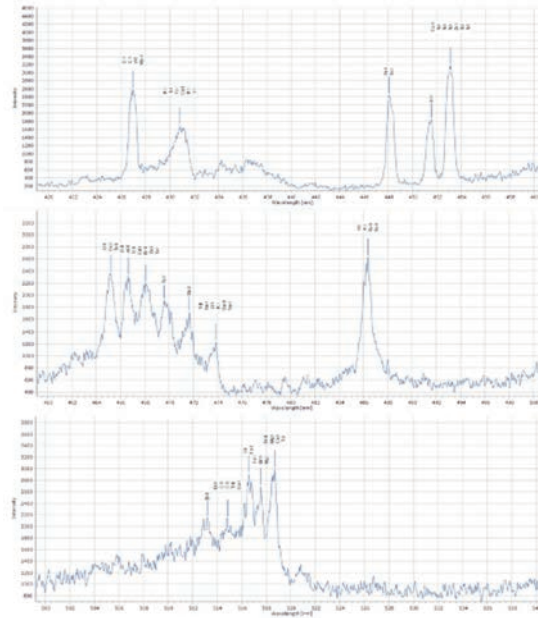


Figure 23. Time-integrated spectra of one cathode shot showing lines from various ionized hydrocarbons.

Computational Research

Our focus here was to address the second ‘goal’ of an HPM device. That is, for the HPM source to operate just as efficiently at a center frequency and on command have that spectral output change to another region. That is to say we wanted to produce a frequency agile/adjustable HPM source. To this end our 3D PIC simulations allowed us to try our ideas without having to build different MILOs. We varied not only the operational parameters of the device such as the voltage but also internal structures like location of beam dumps, size of cathodes to name two, and this led to success on two fronts. We have developed a method for a frequency agile MILO that produces narrowband spectral output not just at its center frequency, but at other discrete frequencies as well. Secondly, this technique also allowed us to reduce the outgassing from internal structures by a factor of 4. This work led to three patent applications.

Figure 24 shows the particle trajectories for one of these configurations at a particular time for our modified MILO while Figure 25 shows the temporal behavior of our modified MILO compared to our canonical MILO. It clearly shows that the temporal behavior is altered only slightly, with very similar peak power but that the spectral output can be varied over a swath of bandwidth.

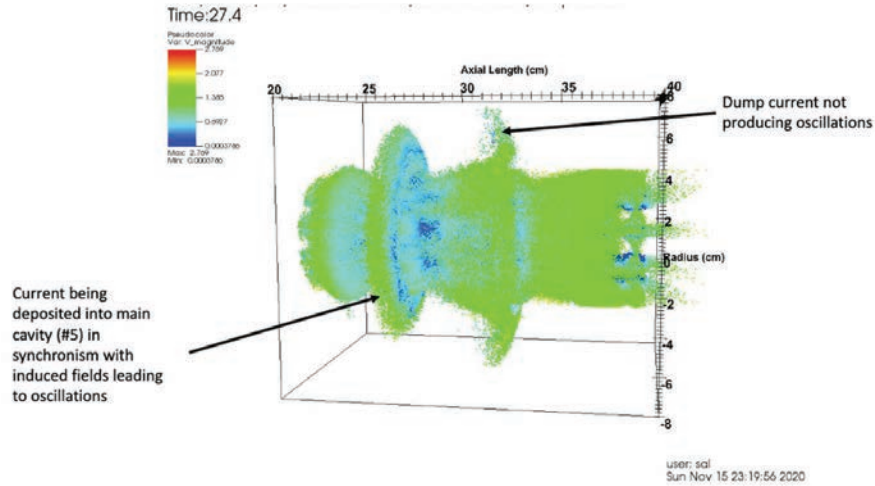


Figure 24. This image is a time slice of particle trajectories in our modified frequency agile MILO.

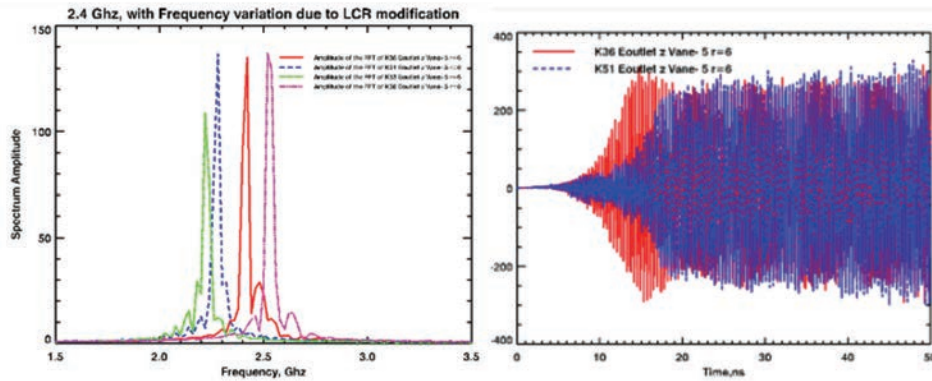


Figure 25. The canonical as well as the frequency agile MILO spectral content and temporal output are shown in the images. Of note is how the spectral output can be varied over some spectral space and that the peak amplitudes remain the same.

Supplemental Task – SOARD-Funded Collaboration with Dr. Rossi, INPE, Brazil

UNM has had a long-standing collaboration with Dr. Jose Rossi's group at INPE, Brazil. These publications appeared/were submitted during the final year of this grant:

- A.F. Teixeira, F.S. Yamasaki, J.O. Rossi, J.J. Barroso, A.F.G. Greco, D.A. Nono, M.C.A. Nono, E.G.L. Rangel, and E. Schamiloglu, "Material Selection for Axial Magnetization of a Gyromagnetic NLTL for Space Applications," *J. Microw. Optoelectron. Electromagn. Appl.*, vol. 20, 629-642 (2021). AFOSR support acknowledged.
- J. Rossi, F. Yamasaki, A. Greco, E. Rangel, J. Barroso, A. Teixeira, L.P. Neto, and E. Schamiloglu, "RF Generation Using a Compact Bench Gyromagnetic Line," *Rev. Sci. Instrum.*, vol. 93, 024704-1-8 (2022). AFOSR support acknowledged.
- R.G. Aredes, E. Antonelli, L.P. Silva Neto, J.O. Rossi, and E. Schamiloglu, "Tunability Behavior of (Ba, Ca)(Zr, Ti)O₃ Ceramic Capacitors Powered by Thermally-Induced Phase Transitions with Applications to Nonlinear Transmission Lines," submitted to *IEEE Trans. Plasma Sci.* (2022). AFOSR support acknowledged.

Conclusions

Considerable progress has been made during this grant period. On the relativistic magnetron, the development of the split cathode – a passive device that leads to electrons being in a squeezed state – has completely eliminated axial leakage current. It also led to much longer pulse durations. The development of new cathodes for the MILO promises more optimal MILO performance. In addition, new techniques for tunable spectral output of the MILO have been demonstrated in PIC simulations.

II. MANAGEMENT SUMMARY

Here is a summary of the personnel who worked on this AFOSR grant:

- Braulio Martinez-Hernandez – U.S. citizen, graduated with M.S.E.E. in December 2020, joined Verus Research (he is now a part time Ph.D. student as well)
- Robert Beattie-Rossberg – U.S. citizen, graduated with B.S. Physics in May 2021; he is currently a Ph.D. student in E.E.
- Eli Bartlit – U.S. citizen, graduated with B.S.E.E. in May 2022, joined SemSol, Albuquerque, NM
- Dmitrii Andreev – U.S. citizen, graduated with Ph.D. in E.E. in May 2022, joined Momentus.Space, San Jose, CA
- Artem Kuskov – U.S. person, graduated with Ph.D. in E.E. in May 2022, joined Verus Research, Albuquerque, NM
- Alex Glick – U.S. citizen, graduated with M.S. in E.E. in May 2022, joined Sandia National Laboratories, Albuquerque, NM (he is now a part time Ph.D. student as well)
- Chris Rodriguez – U.S. citizen, continuing B.S.E.E. student

III. JOURNAL PUBLICATIONS

1. D.A. Andreev, A. Kuskov, and E. Schamiloglu, “Review of the Relativistic Magnetron” (**Featured Article**), *Matter Radiat. Extremes*, vol. 4, 067201-1-19 (2019). AFOSR support acknowledged.
2. J. Leopold, Y. Krasik, Y. Bliokh, and E. Schamiloglu, “Producing a Magnetized Low Energy, High Electron Charge Density State Using a Split Cathode,” *Phys. Plasmas*, vol. 27, 103102-1-9 (2020). AFOSR support acknowledged.
3. Y. Li, M. Liu, C. Liu, J. Feng, E. Schamiloglu, M.I. Fuks, W. Jiang, F. Li, J. Han, and X. Yang, “Mode Control by Rearrangement of the Slow Wave Structure in a 12-Cavity Relativistic Magnetron with Diffraction Output Using Single-Stepped Cavities Driven by a Transparent Cathode,” *AIP Advances*, vol. 11, 035306-1-9 (2021). AFOSR support acknowledged.
4. J.G. Leopold, M.S. Tov, S. Pavlov, V. Goloborodko, Ya.E. Krasik, A. Kuskov, D. Andreev, and E. Schamiloglu, “Experimental and Numerical Study of a Split Cathode Fed Relativistic Magnetron,” *J. Appl. Phys.*, vol. 130, 034501-1-7 (2021). AFOSR support acknowledged.

5. J.G. Leopold, Y. Hadas, Ya. E. Krasik, and E. Schamiloglu, “An Axial Output Relativistic Magnetron Fed by a Split Cathode and Magnetically Insulated by a Compact Low Power Solenoid,” *Trans. Electron Dev.*, vol. 68, 5227-5231 (2021). AFOSR support acknowledged.
6. Y. Li, M. Liu, C. Wang, E. Schamiloglu, C. Liu, M.I. Fuks, W. Jiang, and J. Feng, “PIC Simulation of the Coherent Cerenkov-Cyclotron Radiation Excited by a High-Power Electron Beam in a Crossed-Elliptical Metamaterial Oscillator at S-band,” *IEEE Trans. Plasma Sci.*, vol. 49, 3351-3357 (2021). AFOSR support acknowledged.
7. A.F. Teixeira, F.S. Yamasaki, J.O. Rossi, J.J. Barroso, A.F.G. Greco, D.A. Nono, M.C.A. Nono, E.G.L. Rangel, and E. Schamiloglu, “Material Selection for Axial Magnetization of a Gyromagnetic NLTL for Space Applications,” *J. Microw. Optoelectron. Electromagn. Appl.*, vol. 20, 629-642 (2021). AFOSR support acknowledged.
8. Ya.E. Krasik, J.G. Leopold, Y. Hadas, Y. Cao, S. Gleizer, E. Flyat, Y.P. Bliokh, D. Andreev, A. Kuskov, and E. Schamiloglu, “An Advanced Relativistic Magnetron Operating with a Split Cathode and Separated Anode Segments,” *J. Appl. Phys.*, vol. 131, 023301-1-5 (2022). AFOSR support acknowledged.
9. Y. Li, M. Liu, J. Feng, C. Wang, E. Schamiloglu, C. Liu, and W. Jiang, “PIC Simulations of a Frequency Agile Multicavity Relativistic Magnetron Using Irregular Ring Metamaterials Driven by a Transparent Cathode,” *Phys. Plasmas*, vol. 29, 073107 (2022). AFOSR support acknowledged.
10. J. Rossi, F. Yamasaki, A. Greco, E. Rangel, J. Barroso, A. Teixeira, L.P. Neto, and E. Schamiloglu, “RF Generation Using a Compact Bench Gyromagnetic Line,” *Rev. Sci. Instrum.*, vol. 93, 024704-1-8 (2022). AFOSR support acknowledged.
11. R.G. Aredes, E. Antonelli, L.P. Silva Neto, J.O. Rossi, and E. Schamiloglu, “Tunability Behavior of (Ba, Ca)(Zr, Ti)O₃ Ceramic Capacitors Powered by Thermally-Induced Phase Transitions with Applications to Nonlinear Transmission Lines,” submitted to *IEEE Trans. Plasma Sci.* (2022). AFOSR support acknowledged.
12. Y.P. Bliokh, Ya.E. Krasik, J.G. Leopold, and E. Schamiloglu, “Observation of the Diocotron Instability in a Diode with a Split Cathode,” accepted and to appear in *Phys. Plasmas* (2022). AFOSR support acknowledged.
13. Ya.E. Krasik, S. Pavlov, J.G. Leopold, V. Goloborodko, Y. Hadas, Y.P. Bliokh, and E. Schamiloglu, “A Relativistic S-Band Magnetron with a Split Cathode and Segmented 6-Vane Anode Powered by a Linear Induction Accelerator,” submitted to *J. Appl. Phys.* (2022). AFOSR support acknowledged.
14. K. Ilyenko and S. Portillo, “Upper-Hybrid Oscillations of High-Current Relativistic Electron Beam Under Conditions of Magnetic Self-Insulation,” in preparation for submission to *Phys. Plasmas*. AFOSR support acknowledged.

IV. PATENT APPLICATIONS

1. S. Portillo, “Crossed-Field Frequency Tunability,” patent disclosure submitted December 2020.
2. S. Portillo, “Long Pulse MILO,” patent disclosure submitted December 2020.
3. S. Portillo, “Slatted Frequency Agile Source,” patent disclosure submitted December 2020.